Title

A GCM investigation of dust aerosol impact on the regional climate of North Africa and South/East Asia

Journal

Climate Dynamics, 46(7-8)

ISSN

0930-7575

Authors

Gu, Y
Xue, Y
De Sales, F
et al.

Publication Date

2016-04-01

DOI

10.1007/s00382-015-2706-y

Peer reviewed

Clim Dyn
DOI 10.1007/s00382-015-2706-y

A GCM investigation of dust aerosol impact on the regional climate of North Africa and South/East Asia

Y. Gu[1] · Y. Xue[2] · F. De Sales[2] · K. N. Liou[1]

Received: 24 March 2015 / Accepted: 6 June 2015

Abstract The climatic effects of dust aerosols in North Africa and South/East Asia have been investigated using an atmospheric general circulation model, NCEP/GCM/SSiB (Simplified Simple Biosphere Model) and the three-dimensional aerosol data simulated by the Goddard Chemistry Aerosol Radiation and Transport (GOCART) model. GCM simulations show that due to the scattering and absorption of solar radiation by dust particles, surface temperature decreases over both regions, accompanied by a reduced sensible heat flux. However, precipitation responses are different in these two regions. Due to differences in dust location and the associated heating with respect to the rainfall band and circulation, the effect of dust could either enhance or suppress precipitation. Over the North Africa region where dust particles are mainly located to the north of rainfall band, heating of the air column by dust particles forces a stronger ascent motion over dust layers, which induces an anomalous subsidence (or a weakened upward motion) and suppressed cyclonic circulation to its south where precipitation reduces. Furthermore, both humidity and cloud decrease due to the heating in the middle troposphere (semi-direct effect). In South/East Asia, dust particles are located in the upper troposphere over the major rainfall band during the monsoon season, especially Southwest India and the coastal area of Bay of Bengal. Heating of the air column increases upward motion and strengthens cyclonic circulation. Humidity also increases due to the draw-in of the low level moist air. Therefore, cloud and precipitation increase over South/East Asia associated with dust effect. During the pre-monsoon season, when dust particles are located to the north of the monsoon rainfall band, the heating effect results in shifting precipitation northward. The heating of air column due to dust particles, not surface cooling, plays the major role in precipitation changes. The anomalous upward motion over dust regions will induce a subsidence to its south and subsequently reduce precipitation over that region. Therefore, the responses of circulation and precipitation to aerosol forcing depend on the relative location of dust aerosols with respect to rainfall band, which may explain the fact that contradictory results exist regarding whether the aerosol effect would enhance or suppress precipitation. The dust induced change in precipitation is actually more of redistribution rather than the simple action of increase or decrease.

Keywords Dust · Regional climate · West African monsoon

1 Introduction

Dust particles, which enter the atmosphere through the wind erosion of dry soils, play an important role in the energy balance of the Earth-atmospheric system due to their high emission rate (Andreae 1995; Satheesh and Moorthy 2005; IPCC 2007). Dust sources are most associated with arid regions (mostly topographically low) characterized by little rainfall (annual rainfall under 200–250 mm) (Prospero et al. 2002). The largest dust source region in the world is North Africa (Engelstaedter et al. 2006). Other main source regions are the Middle East, Central and South Asia. The

✉ Y. Gu
gu@atmos.ucla.edu

[1] Department of Atmospheric and Oceanic Sciences, Joint Institute for Regional Earth System Science and Engineering, University of California, Los Angeles, CA 90095, USA

[2] Department of Geography, University of California, Los Angeles, CA 90095, USA

Published online: 19 June 2015

emitted dust from these regions is most persistent (Prospero et al. 2002). The dust emission at the Southern Hemisphere is relatively smaller, but still important for countries such as Australia and Southern Africa. North Africa is heavily influenced by dust with significant year-round dust emissions as shown in the observations derived from the Total Ozone Mapping Spectrometer (TOMS) aerosol index (AI), with maximum emissions from May to August (Engelstaedter et al. 2006). During boreal spring and summer, the air over North Africa is almost permanently loaded with significant amounts of dust (Huang et al. 2013). A large amount of dust particles are carried by the general circulations from North Africa to Europe, Middle East, and across the Atlantic to the southeastern United States, leading to the formation of a major dust belt. In Asia, recurrent dust storms have also emerged as one of the most critical concerns arising from the man-made ecological imbalance in China.

The recent Sahel drought has been recognized as one of the largest climate anomaly at the decadal scale in recent history by the climate research community. Possible causes have been attributed to either land–atmosphere interactions (e.g., Xue and Shukla 1993; Xue 1997; Clark et al. 2001; Taylor et al. 2002) or the sea surface temperature (SST) anomalies in different oceans (e.g., Lamb and Peppler 1992; Rowell et al. 1995; Hoerling et al. 2006). However, several studies have conjectured/suggested that dust can play an important role in the Sahel drought (e.g., Nicholson 2000; Yoshioka et al. 2007; Kim et al. 2010; Zhao et al. 2011). Dust particles absorb and scatter the incoming sunlight and hence influence the radiation field, referred to as the direct radiative effect. Absorbing aerosols, such as dust, play an important role in regional and global climate by heating the air and modifying the horizontal and vertical temperature gradients, atmospheric stability, and convection strength (Miller and Tegen 1998; Menon et al. 2002; Gu et al. 2006). In addition, absorbing aerosols within the cloud may decrease cloud cover by heating the air and reducing relative humidity. However, absorbing aerosols above the cloud may enhance the cloud by the suppression of entrainment due to the increase in temperature above the cloud (Johnson et al. 2004). This leads to either a positive or negative radiative forcing, referred to as the semi-direct effect (Hansen et al. 1997; Gu et al. 2010).

The interactions between dust and other physical processes, such as radiation, cloud, and dynamics, have been found to play an important role in the dust-induced climate change (Yue et al. 2010; Gu et al. 2006). However, there are large uncertainties regarding whether, where, and how the dust enhances or suppresses precipitation. For example, some West African monsoon (WAM) studies have shown that precipitation over North Africa and tropical North Atlantic would be reduced due to dust effects (Miller and Tegen 1998; Biasutti and Giannini 2006; Yoshioka et al. 2007). Using the National Center for Atmospheric Research (NCAR) Community Climate System Model version 3 (CCSM3), Yoshioka et al. (2007) showed that precipitation over North Africa, mainly to the north of the Chad lake, was reduced by direct radiative forcing from specified dust, due to the cooling of troposphere over North Africa in response to radiative forcing of less absorbing dust. Biasutti and Giannini (2006) reported that aerosol could force a meridional gradient in Atlantic SST and hence a drying Sahel based on CMIP3 simulations. Using the National Aeronautics and Space Administration/Goddard Institute for Space studies (NASA/GISS) atmospheric general circulation model (AGCM), Miller and Tegen (1998) examined the climatic effect of dust and found that precipitation had been reduced over the tropical North Atlantic and adjacent continental areas including the Sahel region due to the decreased surface radiation and hence the reduction in evaporation. However, further studies using the same model show opposite results in which precipitation may increase over dry regions of North Africa where dust is originally emitted (Miller et al. 2004). The column warming by dust particles was speculated to cause the increase. Moreover, Kim et al. (2010), using the NASA finite volume general circulation model (fvGCM), found that Saharan dust particles during the boreal summer influence rainfall by heating the lower to middle troposphere, and the rising warm air spawns a large-scale onshore flow carrying the low-level moist air from the Atlantic into the Sahel, leading to increased precipitation to the north of the Chad Lake and decreased rainfall to the south during the monsoon season.

For East Asian region, Menon et al. (2002) investigated the direct radiative effect of aerosols in China and a part of India using the observed aerosol optical depths (AOD) in these regions based on a climate model. They reported that absorbing aerosols could significantly influence the large-scale circulation and hydrologic cycle and may be responsible for the "North Drought/South Flooding" precipitation pattern that frequently occurred in China during the past 50 years. However, Gu et al. (2006) investigated the climatic effects of various types of aerosols in China using an AGCM and suggested that large dust particles in China would heat the air column in the mid- to high latitudes and tend to move the simulated precipitation inland, resulting in less precipitation over southern China (Gu et al. 2006). For South Asia, using the coupled ocean–atmosphere parallel climate model (PCM) developed at the NCAR, Ramanathan et al. (2005) conducted simulations from 1930 to 2000 and found that absorbing aerosols lead to a stronger surface cooling over the Northern Indian Ocean than the Southern Indian Ocean, and hence a weaker South Asian monsoon circulation and reduced precipitation. Lau et al. (2006), however, suggested that the absorption of elevated dust aerosols could lead to intensification of the Indian monsoon through an elevated heating pump mechanism. This

elevated heating pump mechanism of dust aerosols could also enhance the rainfall over the West Africa and Atlantic inter-tropical convergence zone (ITCZ) as shown in their further studies (Lau et al. 2009).

Enhanced precipitation induced by dust effects has also been reported in a few more recent studies over South Asia. Using ICTP-RegCM4, Islam and Almazroui (2012) suggested that dust aerosols may increase the wet season precipitation in Arabian Peninsula. Using the same model, Sun et al. (2012) reported that dust aerosols tend to increase summer precipitation around its source but suppress rainfall in its downwind areas in East Asia. More recently, Vinoj et al. (2014) performed correlation analysis based on satellite data and model simulations and found that dust can heat the atmosphere and induce large-scale convergence over the Arabian Peninsula, leading to increased flow of moisture over India and hence enhanced rainfall. Das et al. (2015) examined the dynamic impact of aerosol direct forcing on the temperature and circulation during the monsoon seasons of 2009 (smaller dust load) and 2010 (larger dust load) in India using a regional climate model RegCM, and reported that aerosols tend to strengthen the summer monsoon zonal wind at 850 hPa over the regions with high AOD values, leading to an increased upward motion over the core monsoon region and hence stronger summer monsoon circulation over India.

Most of the previous studies focus on one particular region and the model results can be controversial on the effect of dust particles on precipitation. It is still not clear why contradict results exist for the same region and how dust aerosols influence the regional climate, especially precipitation, for different regions. The previous studies have generally suggested the two-fold effects of dust aerosols: a heating of the atmosphere that could lead to enhanced precipitation, and a surface cooling that may reduce precipitation. Which of these two effects stands out may depend on model physics and simulated large scale circulation patterns. Furthermore, a recent study on East Asian summer monsoon using WRF-Chem suggested that whether aerosols enhance or suppress precipitation may depend on the location of aerosols with respect to the major rainfall band (Wu et al. 2013).

Given huge uncertainties in the estimate of aerosol climate effect, a better understanding of basic processes, such as how atmospheric circulation patterns respond to warming, appears to be necessary in quantifying present and future changes in climate associated with aerosols (Stevens 2013), especially the absorbing aerosols such as dust which can act as a heat source in the atmosphere. In this study, we will analyze the relationship between dust effects and the local climatology to understand the mechanism of how dust aerosols affect regional circulation patterns and hence precipitation.

The objective of this study is therefore to investigate the impact of dust aerosols on regional climate using recently available dust data with a focus on two different major dust source regions—the North Africa and South/East Asia, by examining the responses of the regional climate system to direct and semi-direct aerosol radiative forcings in the NCEP AGCM model in terms of the temperature, precipitation, cloud, radiation, and general circulation patterns. The organization of this paper is as follows. In Sect. 2, we present the model employed, aerosol data used, and the AGCM experiment design. The model simulations and discussions are presented in Sect. 3. Conclusions are given in Sect. 4.

2 Global dust data, methodology, and model experiment design

Global dust data simulated from the Goddard Chemistry Aerosol Radiation and Transport (GOCART) model was employed in this study. The GOCART (Chin et al. 2009) model uses the assimilated meteorological fields of the Goddard earth Observing System Data Assimilation System (GEOS DAS) to simulate major tropospheric aerosols, including sulfate, dust, black carbon, organic carbon, and sea salt. The GOCART three-dimensional (3D) monthly averages of the dust mixing ratio are available in five bin sizes (0.1–1, 1–1.8, 1.8–3.0, 3.0–6.0, and 6.0–10 μm) with a horizontal resolution of 2° latitude × 2.5° longitude degrees and 72 vertical layers. Single-scattering properties for the various dust size bins are calculated by Mie scattering based on the optical property database in the Global Aerosol Data Set (Köpke et al. 1997). More information on GOCART aerosols is available in Ginoux et al. (2001) and Chin et al. (2002, 2009).

The National Centers for Environmental Prediction (NCEP) AGCM (Kanamitsu et al. 2002) with a horizontal resolution T62 and 17 vertical levels was used in this study. T62 represents 92 longitude equally spaced and 94 latitude unequally spaced grid points, with a horizontal resolution of approximate 1.875° × 1.90° at the equator. The fractional cloud cover used in the radiation calculation is diagnostically determined by the predicted cloud condensate based on the approach of Xu and Randall (1996). The model also has ozone as a prognostic variable with a simple parameterization for ozone production and destruction based on 10-day mean climatological data available from NASA/GSFC. The shortwave (SW) radiation is parameterized following the NASA approach (Chou et al. 1998; Hou et al. 1996, 2002) and the longwave (LW) radiation following the GFDL scheme (Fels and Schwarzkopf 1975; Schwarzkopf and Fels 1991). Both radiation parameterizations use random cloud overlap with shortwave and longwave being called every 1 and 3 h, respectively. The

Simplified Simple Biosphere Model version 2 (SSiB2) has been coupled with this AGCM (Xue et al. 1991, 2004; Zhan et al. 2003) and used in this study, along with the climatological SST.

To increase statistical significance, we have carried out three sets of sensitivity experiments as described below. Each simulation is a 6-year run with the initial condition corresponding to January 1, 2006. Note that for climate simulations, initial condition is not as important. Further more, each experiment contains 6 years of integration with prescribed climatological SST and land processes, representing 6 members starting from different initial conditions.

1. Case CTRL: in the control run (CTRL), the aerosol is turned off, therefore the aerosol effect is excluded from model simulation.
2. Case 1984 (C1984): in the second experiment, the aerosol effect is accounted for by incorporating the GOCART dust data for Year 1984, representing a drier year with a large dust AOD.
3. Case 2003 (C2003): the third experiment is identical to (2), except that the GOCART dust data for Year 2003 is used, representing relatively wetter years with relatively small dust AOD.

The cases in this study are based on the experimental design of the West African Monsoon Modeling and Evaluation Experiment II, which investigates the effects of external forcing, such as SST, land use and land cover change, and aerosol, on the Sahel drought during the 1980s (Xue et al. 2015). Based on the observations, the West Africa during the 1980s had the most severe drought in the world in the last century and the South/East Asia also suffered the drought. Meanwhile, there were more dust emissions and loadings over North Africa and South/East Asia during that period. On contrast, the 2000s became relatively wetter with less dust aerosols (Redelsperger et al. 2006). Experiments C1984 and C2003 are therefore designed to represent the 1980s and the 2000s conditions, respectively, to test the effect of different dust loadings on regional climate anomaly, such as precipitation, surface temperature, etc. We also performed a CTRL case in which aerosol direct and semi-direct effects are excluded to more clearly see the significant dust effects.

Since the three sets of experiments are identical except for the prescribed aerosols, significant differences in the ensemble mean between the three sets of experiments can be attributed to the sensitivity of the regional climate responses to aerosol radiative forcing. The two-tailed Student's *t* test, in which deviations of the estimated parameter in either direction are considered theoretically possible, is used in this study to measure the statistical significance of the sensitivity simulations. The threshold chosen for statistical significance is 0.1 for all the results in this study.

3 Model simulations

Figure 1 illustrates the monthly mean GOCART dust aerosol optical depth (AOD) for the Year 1984. The spatial and temporal variations are consistent with those analyses based on observation as discussed in the Introduction. It clearly shows the major dust belt which extends from North Africa to Middle East, Central and South Asia, and across the Atlantic to the southeast United States. AOD appears to have the largest magnitude over North Africa and Asia during June–July–August (JJA), in agreement with that reported by Engelstaedter et al. (2006) based on TOMS observations. The center of AOD jumps northward in May due to the onset of West Africa monsoon and the occurrence of precipitation over Sahel, leading to less dust emission in this semi-arid region. Dust aerosols also appear in Australia during boreal winter time, but the AOD magnitude is much smaller compared to the major dust belt. Since the dust AOD shows the largest values during JJA and the monsoon period spanning over May–September, we have focused our analysis over June to September (JJAS). Figure 2a, b show the JJAS mean AOD differences between C1984 and CTRL and C1984 and C2003, respectively. Compared to C2003, more dust aerosols were found in 1984 over North Africa and Atlantic, Arabian Sea and Middle East, and South and East Asia (India and China). The dust AOD center is located around 15°N–30°N (Fig. 2b). Figure 2a shows similar patterns as in Fig. 2b, but with a larger magnitude and larger area of differences because CTRL does not include dust aerosols in the simulation.

Besides the scattering of solar radiation like many other aerosols, dust aerosols, especially those in larger size, also substantially absorb solar radiation. Figure 3 shows the JJAS mean differences in the total solar heating (Fig. 3a, b) and the surface downward fluxes (Fig. 3c, d) between C1984 and CTRL, and C1984 and C2003, where the contours are plotted only for differences which are statistically significant at a significance level of 0.1. Atmospheric column heating (Fig. 3a, b), which is well correlated to differences in the dust aerosol AOD (Fig. 2), is consistent with dust aerosol concentration due to the absorption of solar radiation by dust particles with maximum values above 1 K day^{-1} over North Africa, Middle East, South Asia, and China. The corresponding surface downward fluxes are reduced over dust regions as a combined result of the scattering and absorption of solar radiation by dust particles (Fig. 3c, d). Similar to Fig. 2, differences between C1984 and CTRL are larger than those between C1984 and C2003 related to much larger differences in AOD, but the overall patterns look similar.

Changes in radiative heating alter the atmospheric thermal structure and the energy and water balances of the

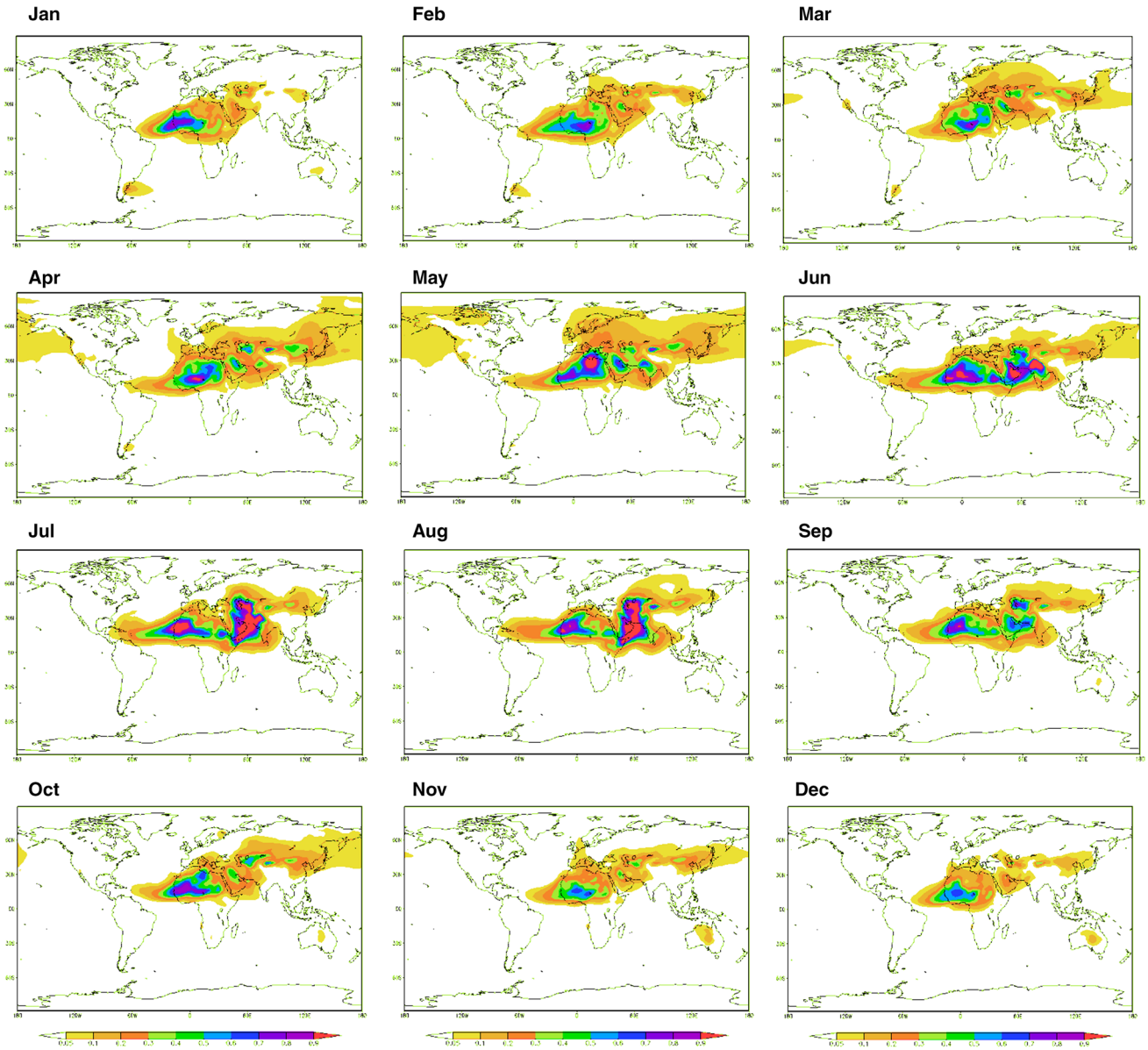

Fig. 1 Global monthly mean AOD simulated from GOCART for 1984

earth-atmosphere system. Figure 3 clearly indicates that the areas with main aerosol impacts cover two major monsoon system regions: the North Africa and tropical north Atlantic region and the South/East Asia region. In the following discussion, we focus on dust aerosol effects on these two regions' climate. One major difference between these two regions is that the West Africa monsoon is weaker than the South/East Asia monsoon counterpart due to different large-scale circulation patterns. Figure 4 shows the global JJAS mean precipitation simulated from CTRL (Fig. 4a) and the corresponding observations (Fig. 4b) obtained from CPC Merged Analysis of Precipitation (CMAP), both illustrating the stronger monsoon precipitation over the South/East Asia than that over the North Africa. Another difference is that over North Africa, dust aerosols are located to the north of the rainfall band. Over South/East Asia, dust aerosols are located where precipitation occurs.

3.1 Impact of dust on summer climate of North African and Atlantic

The monsoon system, which is critically important in providing water for agriculture activities in a number of Earth's most populous regions, has not been adequately modeled in the past. Differential heating of the land and the

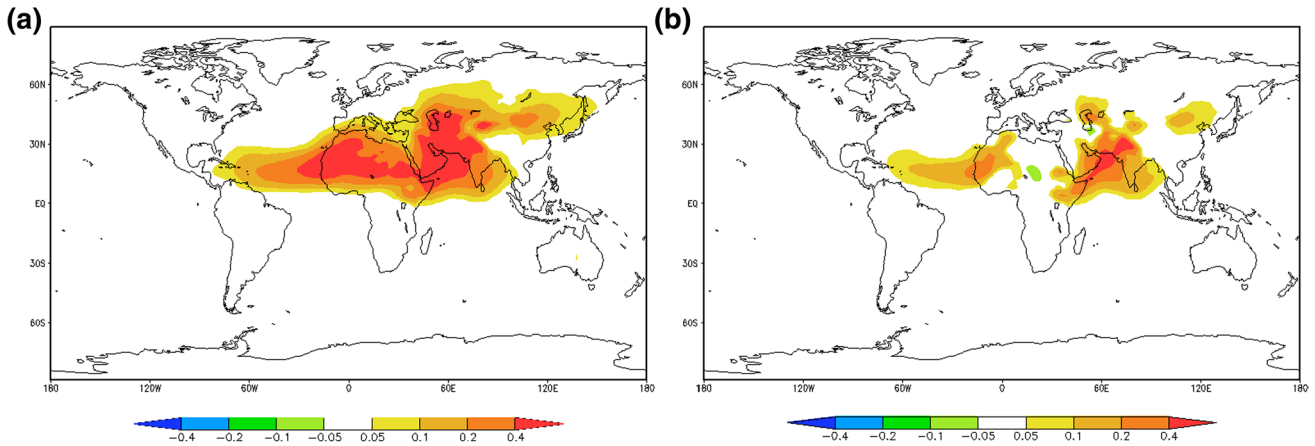

Fig. 2 Global JJAS differences in dust AOD between **a** C1984 and CTRL, and **b** C1984 and C2003

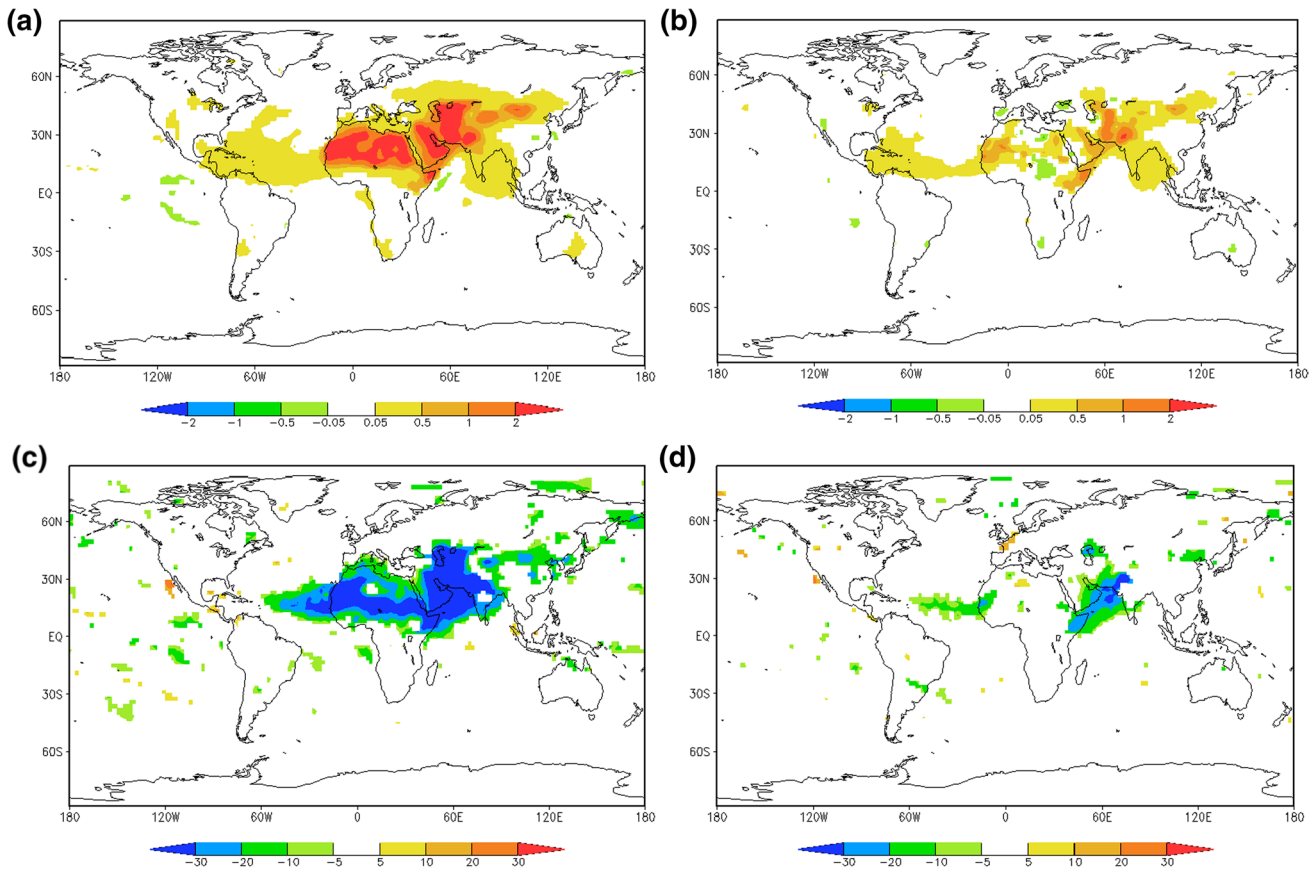

Fig. 3 Global JJAS mean differences in solar heating (K day^{-1}) between **a** C1984 and CTRL, and **b** C1984 and C2003; JJAS mean differences in surface downward solar flux (W m^{-2}) between **c** C1984 and CTRL, and **d** C1984 and C2003. Differences which are statistically significant at a significance level of 0.1 are *color shaded*

ocean is considered to be one of the important factors that determine the strength, duration and spatial distribution of large-scale monsoons (Webster et al. 1998; Xue et al. 2004). In this section, we investigate how the dust heating affect the WAM which is relatively weak compared to the Asian monsoon (Griffiths 1972). Figure 5 shows the JJAS mean differences in surface temperature over North Africa between C1984 and CTRL, and C1984 and C2003, where dots represent differences that are statistically significant at a significance level of 0.1. Note that the SST forcing is the

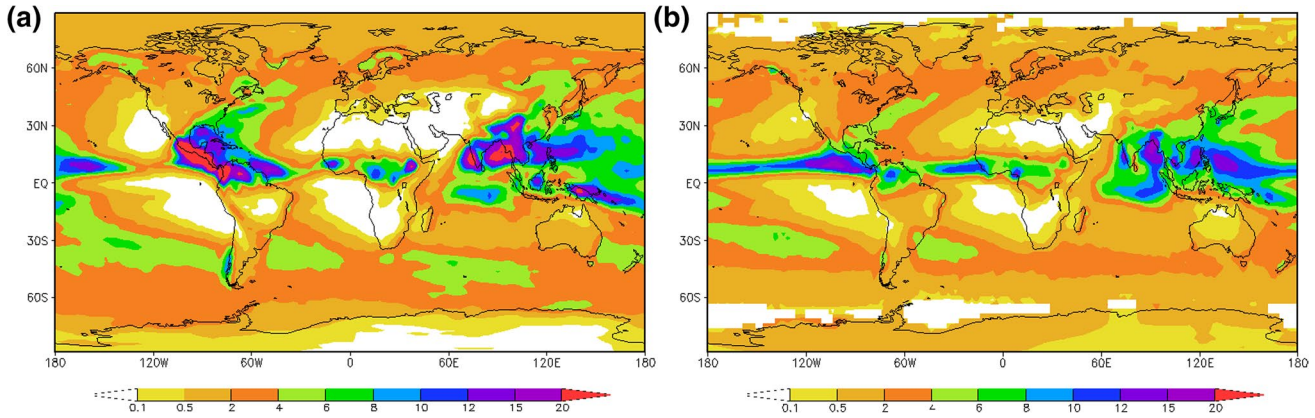

Fig. 4 Global JJAS mean precipitation (mm day^{-1}) **a** simulated from CTRL, and **b** observations from CMAP

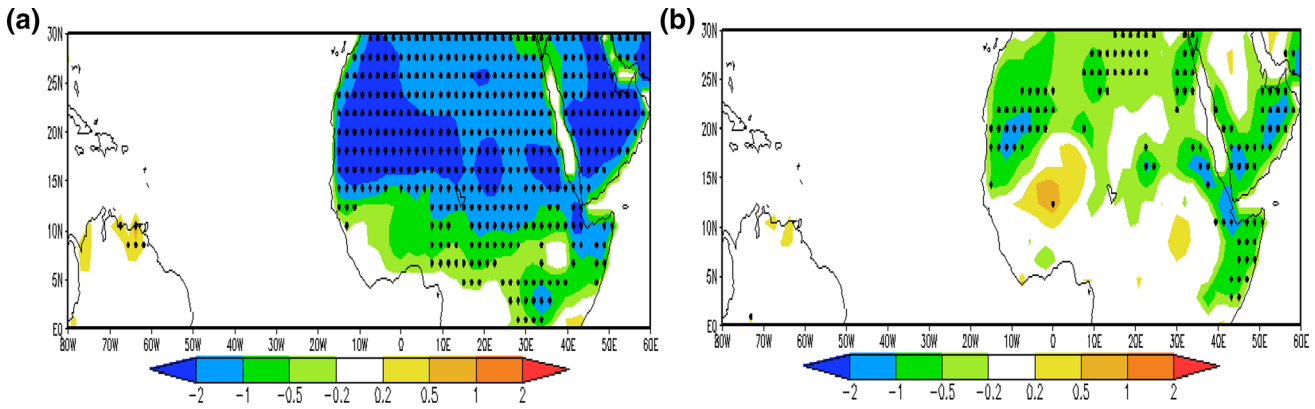

Fig. 5 JJAS mean differences in surface temperature (K) between **a** C1984 and CTRL, and **b** C1984 and C2003 for North Africa and tropical north Atlantic. The *dotted area* denotes differences which are statistically significant at a significance level of 0.1

same in these cases so there is no change of surface temperature over the Atlantic. Due to the scattering and absorption of dust aerosols in the atmosphere and the consequence of reduced net solar flux at the surface, surface temperature decreases over North Africa where dust aerosols are located. Figure 5a, b have similar spatial patterns; however, Fig. 5a shows much larger magnitude and spatial extent of the areas with significant temperature differences, consistent with the heating difference discussed in the previous section. Figure 6 shows the JJAS mean precipitation from CTRL and differences between C1984 and CTRL, and C1984 and C2003. Major monsoon precipitation (Fig. 6a) occurs over West Africa and tropical north Atlantic between equator and about 15°N (ITCZ), located to the south of the dust belt, which is mainly located between 15°N and 30°N. Due to the dust effect, precipitation is reduced over West Africa, the coastal region of Central Africa, and tropical north Atlantic (Fig. 6b, c). Again, differences between C1984 and CTRL, which represent the extreme effect produced by dust aerosols, display a larger magnitude and cover more broad areas. The area with major precipitation differences over West Africa is located to the south of the dust band. Meanwhile, the tropical Atlantic also shows a substantial precipitation reduction, although the aerosol change there is marginal (Fig. 2). An important feature of the WAM is the low level moisture transfer. During the WAM season, northwestward flow across the Guinean coast curves northeastward then eastward and brings moisture into West Africa, which is a critical WAM feature (Xue et al. 2010). Figure 7 shows the longitude-height cross-section of JJAS mean differences in zonal wind (Fig. 7a) and streamline and temperature (Fig. 7b) between C1984 and CTRL at 10°N. The anomalous westerly flow is found off the coast of West Africa with a maximum near 30°W (Fig. 7a), which increases moisture transport from the central and eastern Atlantic, producing enhanced rainfall over the coastal area of West Africa while suppressing rainfall over the western and central Atlantic. The anomalous large-scale circulation features a rising motion over the eastern Atlantic and West Africa and a sinking motion over the

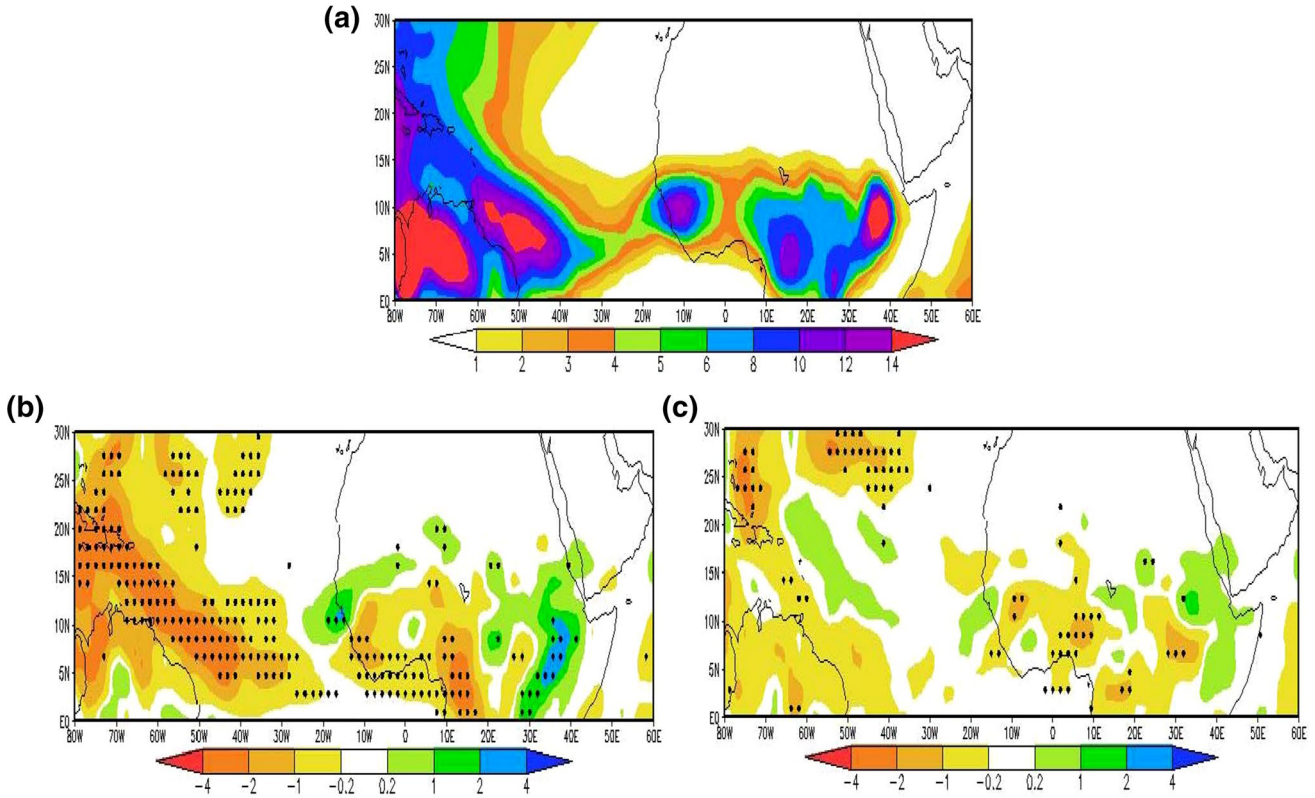

Fig. 6 **a** JJAS mean precipitation (mm day^{-1}) simulated from CTRL, and JJAS mean differences in precipitation between **b** C1984 and CTRL, and **c** C1984 and C2003 for North Africa and tropical north Atlantic. The *dotted area* denotes differences which are statistically significant at a significance level of 0.1

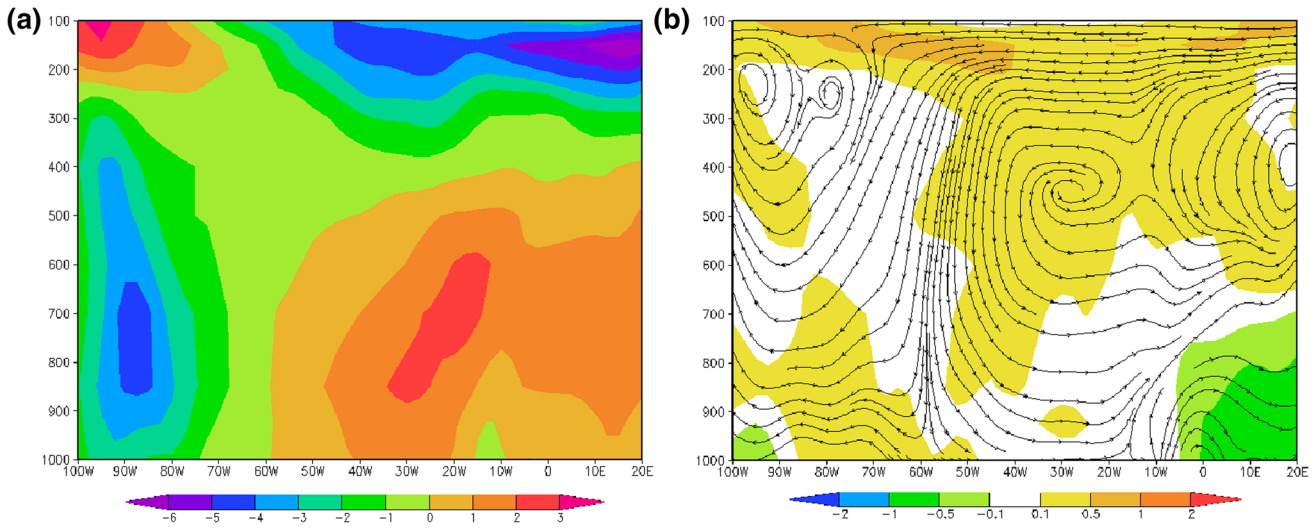

Fig. 7 Longitude-height cross section of JJAS mean differences in **a** zonal wind (m s^{-1}) and **b** streamline (u; $-\omega \times 100$) and temperature (K, *shaded*) between C1984 and CTRL at 10°N

central and western Atlantic (Fig. 7b). This is in agreement with the finding by Lau et al. (2009) in which the reduced precipitation is due to an anomalous Walker circulation with a stronger rising motion over the West Africa land. Since the spatial patterns are similar in Fig. 6b, c with a much stronger signal depicted in the former figure, we will focus on differences between C1984 and CTRL in the following analysis.

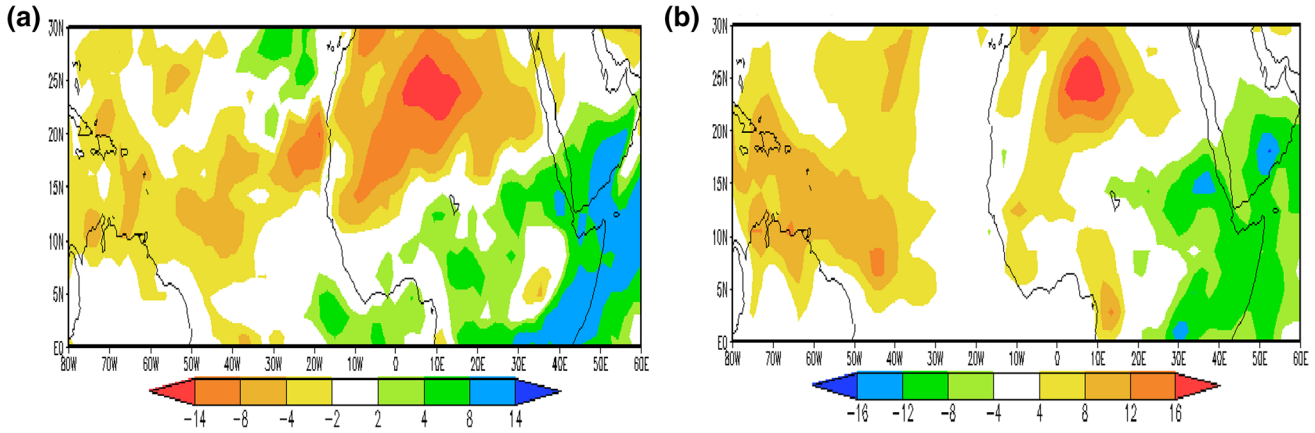

Fig. 8 JJAS mean differences in **a** total cloud cover (%) and **b** OLR (W m^{-2}) between C1984 and CTRL for North Africa and tropical north Atlantic

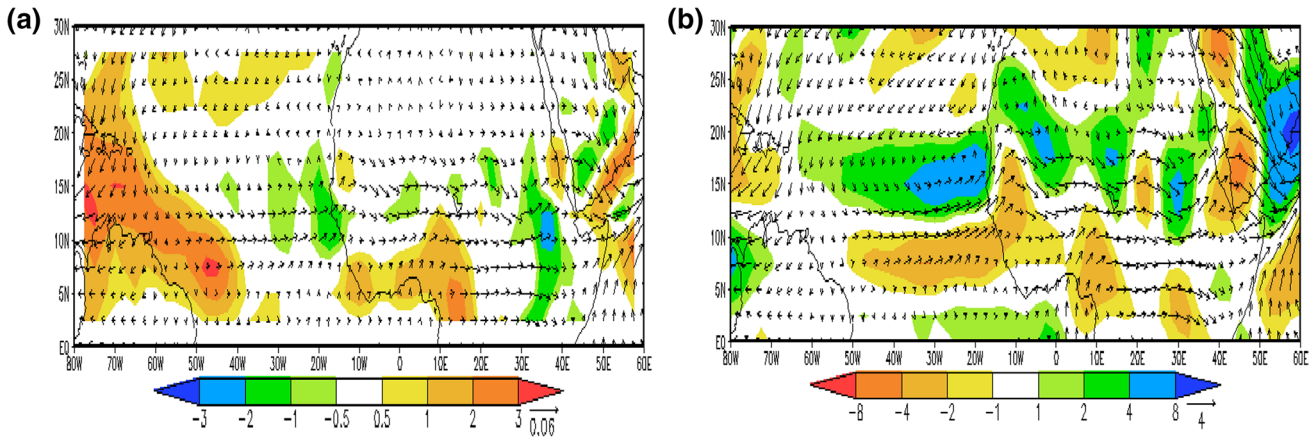

Fig. 9 JJAS mean differences in **a** moisture flux (m s^{-1}) at 850 hPa and vertically integrated moisture flux divergence (mm day^{-1}), and **b** 850 hPa wind (m s^{-1}) and vorticity (10^{-6} s^{-1}) between C1984 and CTRL for North Africa and tropical north Atlantic

Figure 8 shows differences in the total cloud cover and outgoing longwave radiation (OLR). The total cloud cover experiences decreases over the North Africa and north Atlantic dust regions in association with the heating generated by dust particles (referred to as the semi-direct effect), while increases in cloud cover is found to the south of the North African dust band, including the Gulf of Guinea (Fig. 8a). The reduced cloud cover in North Atlantic is generally consistent with the reduced precipitation there (Fig. 6b). OLR increases over the dust region associated with less cloud (Fig. 8b). Near the coastal Gulf of Guinea, the OLR increase corresponds to the reduced precipitation, indicating weakened convection (Figs. 6b, 8b).

To better understand changes in precipitation, we further analyze differences in the summer circulation between C1984 and CTRL. Figure 9 illustrates differences in the JJAS mean moisture flux at 850 hPa and the vertically integrated moisture flux divergence, as well as wind and vorticity at 850 hPa. Over the northern Africa, where dust heating prevails (Fig. 2a), the positive vorticity and cyclonic circulation are produced (Fig. 9b). However, the atmosphere is rather dry over the Sahara desert (Fig. 10a), and no substantial change in moisture flux convergence there is found (Fig. 9a). Only at the southern boundary of this area and the eastern North Atlantic, where the moisture is relatively high, there is an increase in moisture flux convergence and precipitation. Overall, such an increase is relatively small. To the south of the area with positive vorticity difference and enhanced convergence, the reduced rainfall over West Africa is consistent with the reduced moisture flux convergence (Fig. 9a) and a weakened cyclonic circulation in the low atmosphere at 850 hPa (Fig. 9b).

The relative humidity has the maximum value over about 10°N (Fig. 10a), corresponding to precipitation

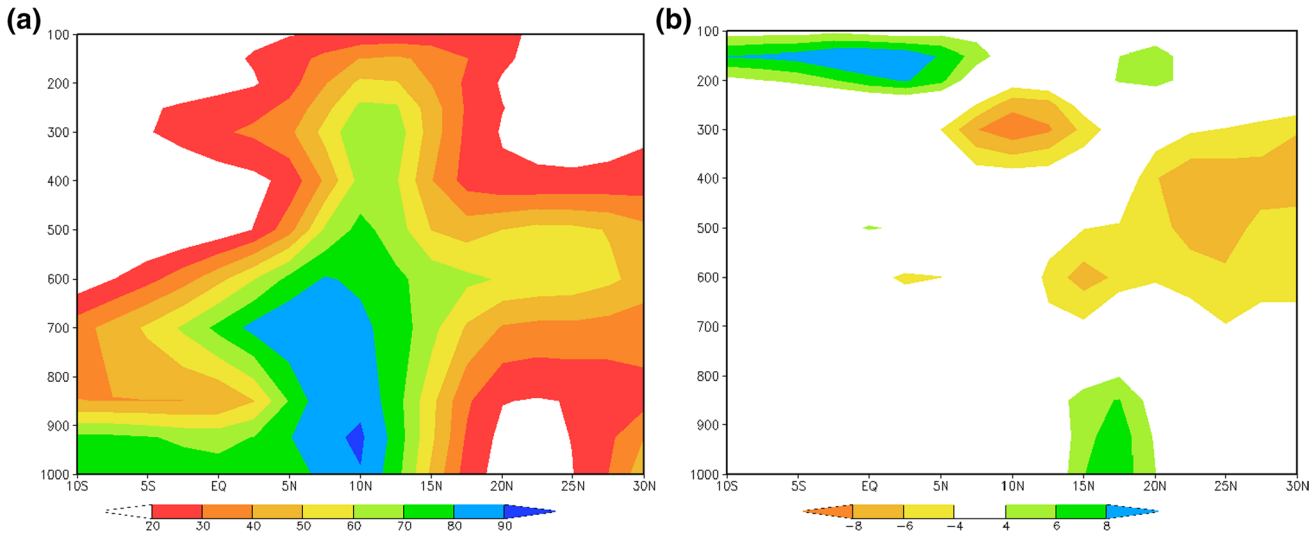

Fig. 10 Latitude-height cross section of JJAS mean **a** relative humidity (%) simulated from CTRL, and **b** its difference between C1984 and CTRL at 10°W

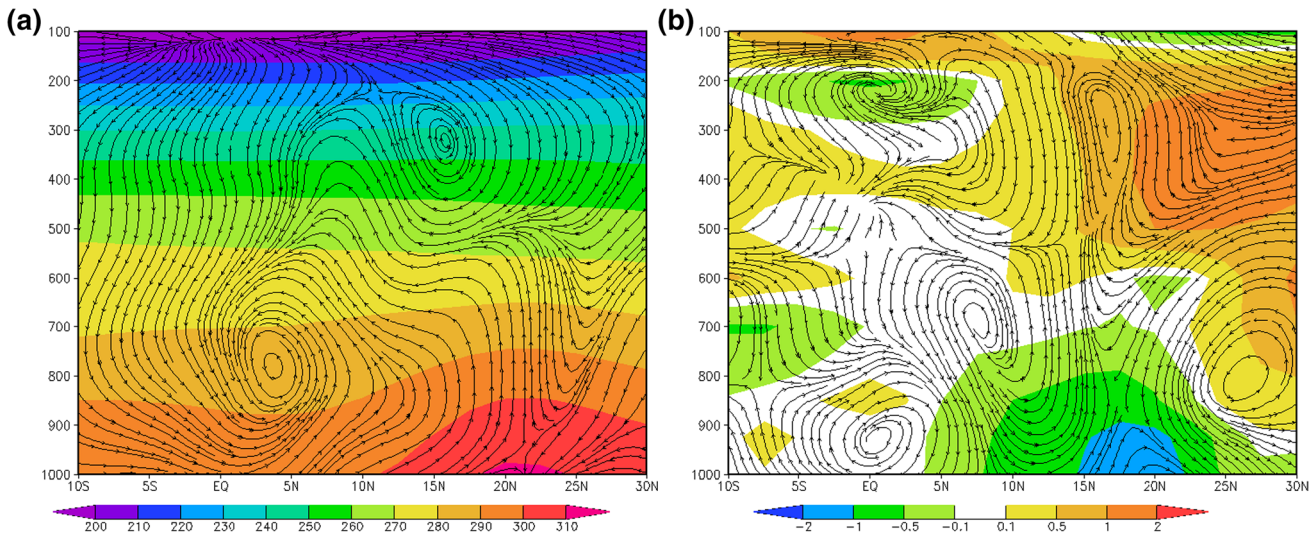

Fig. 11 Latitude-height cross section of JJAS mean **a** streamline (v; $-\omega \times 100$) and temperature (K, *contour*), and **b** their differences between C1984 and CTRL at 5°E

center (Fig. 6a). Due to the heating of air by dust particles and the subsequent semi-direct effect, the relative humidity over 10°–25°N in the middle troposphere is reduced (Fig. 10b), leading to less cloud cover over that region (Fig. 8a). Although the relative humidity in the lower troposphere over the rainfall band is slightly enhanced due to the colder surface temperature (Fig. 10b), the reduced upward motion or suppressed convection (Fig. 11b) is dominant, which will be discussed in the next section. The semi-direct effect or warming over North Africa leads to decreased cloud cover and hence less reflected solar radiation, which is a positive forcing opposite to the direct effect. However, the direct dust aerosol effect exceeds the semi-direct effect in this case, leading to less downward solar fluxes at the surface (Fig. 3c) and colder surface temperatures (Fig. 5a).

To further delineate changes in circulation and relevant mechanisms caused by the aerosol forcing, we show the latitude-height cross sections of JJAS mean temperatures and streamlines at 5°E, for CTRL and differences between C1984 and CTRL (Fig. 11). Due to higher temperature over the land surface, the monsoon inflow is seen near the surface at about 5°N and extends to about 20°N

confined below 850 hPa, with ascending motion across these latitudes. Much of this flow feeds into the deep ITCZ convection between 5°N and 15°N where major precipitation occurs. The upward motion below 600 hPa around 15°N–25°N is constrained by the anticyclonic circulation of the Saharan high, which produces subsidence in the upper troposphere (200 –600 hPa) and acts as the north barrier of the WAM. The intersection of the deep tropical system (~5°N–15°N) and the shallower subtropical system to the north (~15°N–25°N) results in a southward tilt of the stream lines in the middle troposphere. Three southward flows are seen over the summer North Africa. One occurs close to the surface and to the north of 20°N where southward flow converges with the northward flow and rises over the continental thermal low. This southward flow generates the easterly wind under Coriolis forces known as Harmattans that lifts the dust from the dry surface. The second southward flow occurs in the middle troposphere at about 15°N as a part of the Saharan high, which produces the African easterly jet (AEJ). The third southward flow is seen at ~200–250 hPa over the region of deep convection (~5°N–10°N) corresponding to the tropical easterly jet, and large-scale subsidence occurs south of 5°N (Fig. 11a). These simulated circulations agree well with the observed major circulation features of the WAM reported by Cook and Vizy (2006) based on NCEP reanalysis climatology averaged over JJAS for 1949–2000. When dust aerosols present, they heat the upper atmosphere, with maximum temperature changes occurring at about 300 hPa over the North African desert region around 25°N; meanwhile, to the north of 10°N the surface shows cooling due to less downward solar radiation reaching the surface as discussed for Fig. 3c. The heating source induces an increased upward motion and generates a divergence around 25°N in the upper atmosphere because the air cannot go further up being capped by the tropopause (Fig. 11b), where it is too dry and hence precipitation cannot be produced by the enhanced air ascent. By air continuity, the divergence in the upper troposphere and the enhanced upward air movement induces a descent to its south, where downward motion anomalies are found above 500 hPa from 5°N to 15°N, together with an anomalous overturning near the surface, with an anomalous uplift around 15°N and downward anomalies from 5°N to 10°N, weakening the rainfall there (Fig. 6b). Meanwhile, to the north at about 20°N–25°N, the heating source generated by dust directly forces a baroclinic signal in which the higher level divergence corresponds to a lower level convergence over Sahara and northern Sahel (Fig. 11b). The changes in circulation also show stronger/weakened southward flow at 550 hPa/200 hPa, which would in turn enhance/weaken the AEJ/tropical easterly jet, respectively, which is consistent with the climate feature in the Sahel dry years (Xue and Shukla 1993). The stronger AEJ is associated with the heating to its north by the dust particles, which would result in a stronger AEJ or a southward shift of its location favoring more precipitation over the Guinea Coast region and less precipitation over the Sahel (Cook 1999). In this study, the changes in moisture flux divergence (Fig. 9a) and precipitation over the West Africa monsoon region (Fig. 6b) are consistent with the AEJ change. However, if the simulated WAM inflow was strong enough to extend further northward, the Sahel may get more precipitation (e.g., Miller et al. 2004).

3.2 Impact of dust on summer climate of South/East Asia

The Asian monsoon system, which consists of Indian monsoon and East Asian monsoon and covers India, China, Indochina, as well as other surrounding countries and nearby oceans, is the major monsoon system in the world, (Flohn 1957; Ding 1994). In this section, we discuss how the dust aerosols affect the regional climate in South/East Asia. Due to both the scattering and absorption of solar radiation by the dust particles, surface temperature and sensible heat fluxes show negative changes over the India and the coastal area of the Bay of Bengal, as well as over the northern China (Fig. 12a, b), where the dust aerosols are located (Fig. 2a), similar to the temperature response in the North Africa and Atlantic region (Fig. 5a). However, a surface warming is induced over and around the Tibetan Plateau area because the heating due to dust aerosols occurs in the middle to upper troposphere over that area due to the elevated topography (Fig. 15b), as also shown in Lau et al. (2006). Warming is also induced over southeastern China associated with the anomalous southerly carrying warmer and moist air from the ocean which will be discussed later.

Figure 13 shows the JJAS mean precipitation simulated from CTRL and the differences between C1984 and CTRL. During the monsoon season, major precipitation band over South and East Asian continent and surrounding oceans shows a southwest-northeastern orientation with the maximum located over the southwest of India and the Bay of Bengal (Fig. 13a). The dust aerosol effect increases precipitation significantly along this monsoon rainfall band, with the maximum increase over the coastal area of the Bay of Bengal and the northwest India. A few other studies also reported that excessive monsoon rainfall is concentrated over the same area (Lau et al. 2006; Islam and Almazroui 2012; Vinoj et al. 2014). Although the areas with significant precipitation increase are generally consistent with the dust regions, the rainfall change in China has no substantial dust AOD difference (Fig. 2). The induced changes in circulation due to the aerosol effect play a role here. Meanwhile there is decreased rainfall to the south of the increasing precipitation band mostly over

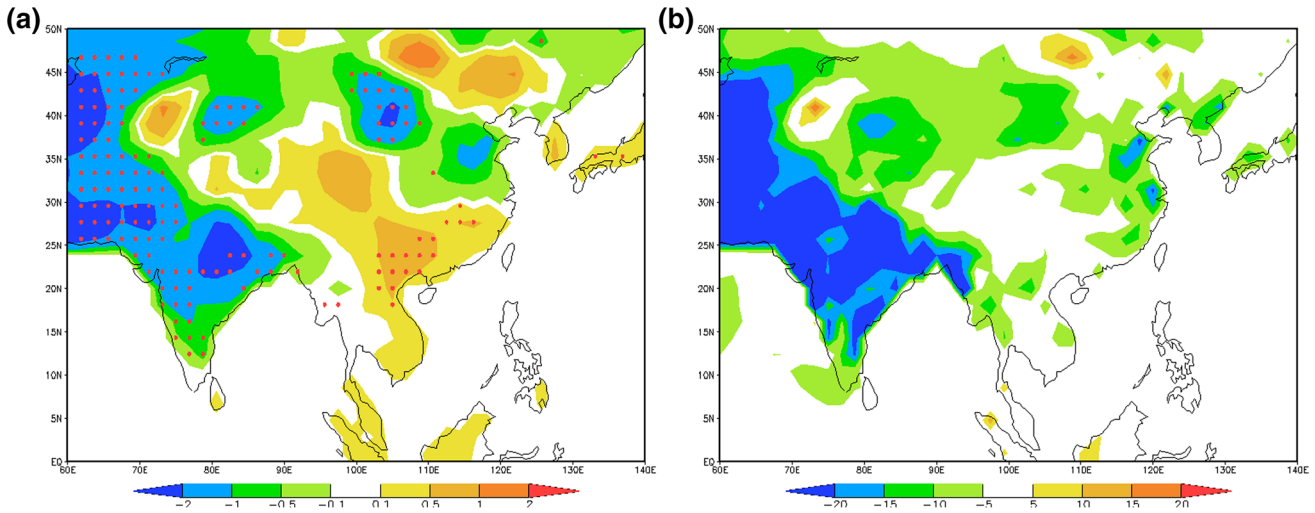

Fig. 12 JJAS mean differences in **a** surface temperature (K) and **b** surface sensible heat flux (W m^{-2}) between C1984 and CTRL for South/East Asia. The *dotted area* denotes differences which are statistically significant at a significance level of 0.1

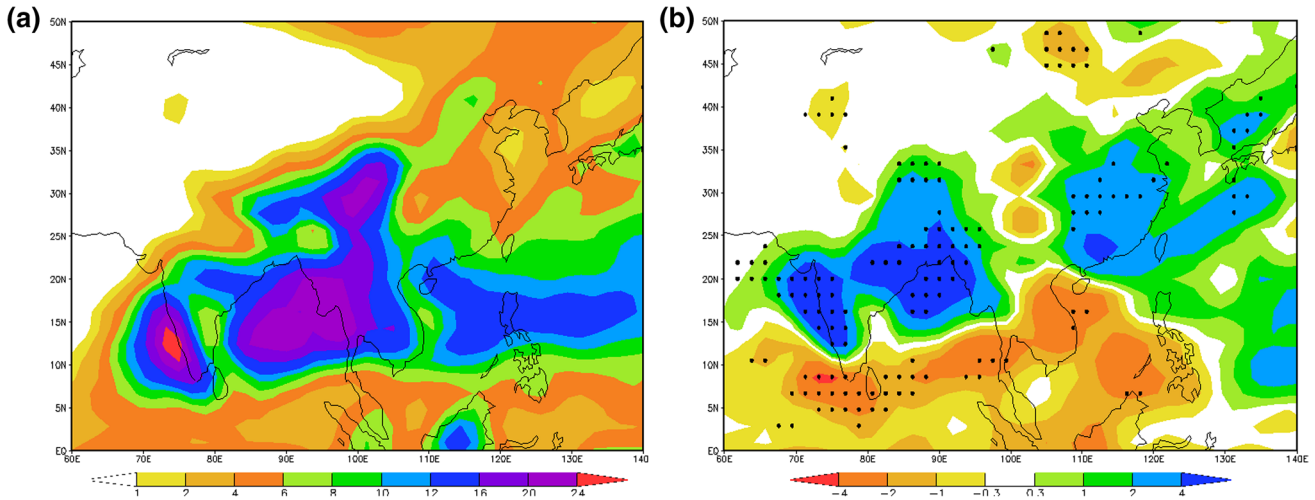

Fig. 13 **a** JJAS mean precipitation (mm day^{-1}) simulated from CTRL and **b** JJAS mean differences in precipitation between C1984 and CTRL for South/East Asia. The *dotted area* denotes differences which are statistically significant at a significance level of 0.1

oceans, forming a dipole pattern. The increased precipitation well corresponds to increased cloud (Fig. 14a) and decreased OLR over this region (Fig. 14b) which indicates a stronger convection.

Cross-sections of JJAS mean temperature and streamlines at 90°E, where one of the maximum precipitation changes is located over Bay of Bengal, for CTRL and the differences between C1984 and CTRL are given in Fig. 15. Due to the strong warm land temperature north of 20°N during JJAS, monsoon inflow is seen at equator and extends to about 25°N and associated with a large region of upward motion between 10°N and 35°N (Fig. 15a), where the major rainfall occurs (Fig. 13a). All the monsoon flow feeds into the deep convection that goes all the way up to tropopause (Fig. 15a). Due to the dust heating of the upper atmosphere (~200 hPa) over 15°N–40°N (Fig. 15b), where the Tibetan Plateau is located, increased upward air movement is broadly found between 15°N and 35°N, which induces convergence in the lower atmosphere and draws more low-level moist air from the ocean into the land, leading to a convergence of moisture flux (Fig. 16a), in agreement with the elevated heat pump theory suggested by Lau et al. (2006) and also reported by Gu et al. (2006). Meanwhile, stronger sinking to the south of rising region between the equator and 10°N is induced, leading to decreased precipitation over that region.

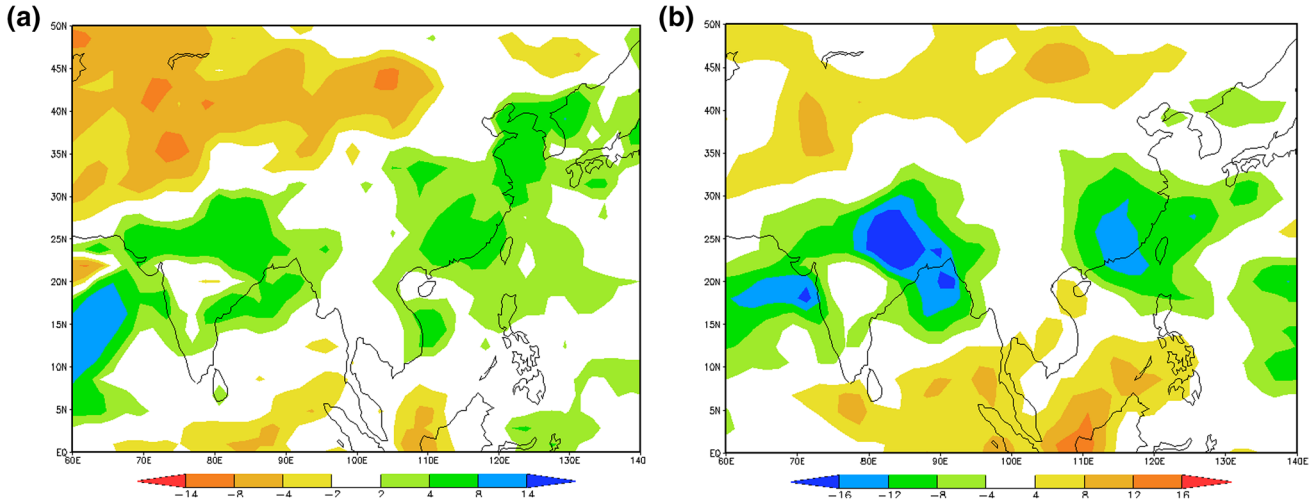

Fig. 14 JJAS mean differences in **a** total cloud cover (%) and **b** OLR (W m^{-2}) between C1984 and CTRL for South/East Asia

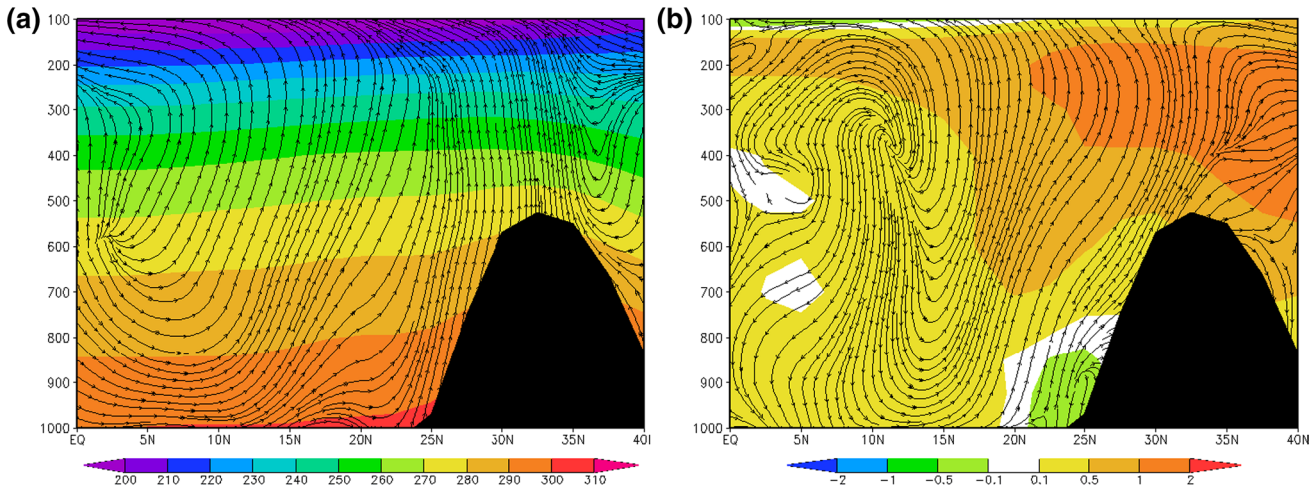

Fig. 15 Latitude-height cross section of JJAS mean **a** streamline (v; −w × 100) and temperature (K, *contour*), and **b** their differences between C1984 and CTRL at 90°E

Figure 16 illustrates the spatial differences in moisture flux at 850 hPa and the vertically integrated moisture flux divergence, and wind and vertical velocity at 850 hPa over South/East Asia, consistent with the circulation change in Fig. 15. Corresponding to the increased precipitation (Fig. 13b), stronger moisture flux convergence is found over the northwest India and the coastal area of Bay of Bengal (Fig. 16a). Furthermore, the stronger monsoon flow also brings in more moist and warmer air to the eastern China (Fig. 16a), leading to the surface warming (Fig. 12a) and enhanced precipitation (Fig. 13b) there although there is no aerosol dust change. Vertical velocity differences show that upward motion is enhanced over these regions at 850 hPa, companied by a decreased upward velocity to its south (Fig. 16b). Figure 17a, b show the relative humidity from CTRL and the differences between C1984 and CTRL. High relative humidity is found between 5°N and about 30°N (Fig. 17a), corresponding to the major precipitation band (Fig. 13a). Due to dust heating effect in the upper atmosphere, the strengthened upward motion draws in more low-level moist air and enhances the relative humidity (Fig. 17b), cloud (Fig. 14a), and precipitation (Fig. 13b) over this region. The dust semi-direct effect hence leads to a negative forcing to the surface temperature changes similar to the aerosol direct effect. Our finding is in agreement with Vinoj et al. (2014) who found that West Asian dust enhances monsoon rainfall in India. The increase in precipitation over South/East Asia due to dust effect appears to be opposite from the decrease in precipitation over the North Africa and tropical north Atlantic region. The responses of

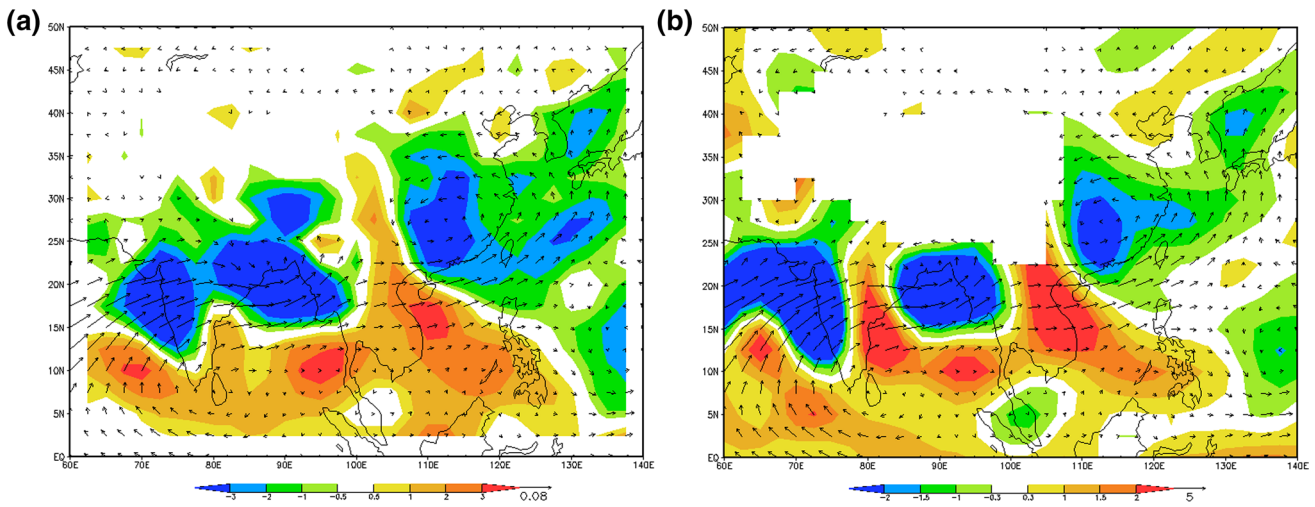

Fig. 16 JJAS mean differences in **a** moisture flux (m s^{-1}) at 850 hPa and vertically integrated moisture flux divergence (mm day^{-1}), and **b** 850 hPa wind (m s^{-1}) and vertical velocity (10^{-2} Pa s^{-1}) between C1984 and CTRL for South/East Asia

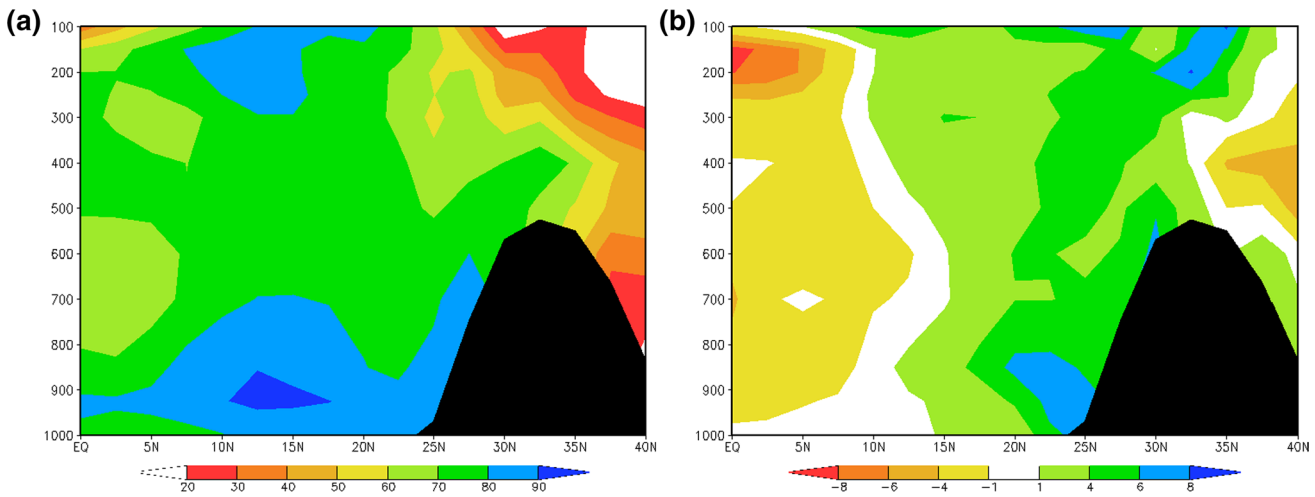

Fig. 17 Latitude-height cross section of JJAS mean **a** relative humidity (%) simulated from CTRL and **b** its difference between C1984 and CTRL at 90°E

circulation to the dust aerosol effect are also different for those two monsoon regions.

3.3 Discussions on different characteristics of dust effects over North Africa and South/East Asia

It is shown from above model results that the dust aerosol effects on precipitation over the North Africa and over South/East Asia show very different characteristics. One major difference between the two monsoon regions is that the WAM is weaker with monsoon inflow extending from 5°N to 20°N, while the South/East Asia monsoon is much stronger, covering a broad area from equator to about 35°N. Another feature about South Asia monsoon is the existence of Tibetan Plateau, which helps to strengthen the ascent motion of the air. The main difference in AOD field over these two regions is that in North Africa, the JJAS dust aerosols are mainly located to the north of the major monsoon rainfall band, while in South/East Asia, the dust aerosols are located over the region that covers monsoon precipitation. In both cases, the relative rising motion is produced in the dust region due to the heating of air by dust aerosols (Gu et al. 2006; Lau et al. 2006, 2009). Consequently the subsidence located to the south of the dust region is induced. However, such changes in circulation produce very different precipitation anomaly patterns in these two major monsoon regions. In the case of North Africa, the enhanced relative upward motion over the Sahara Desert

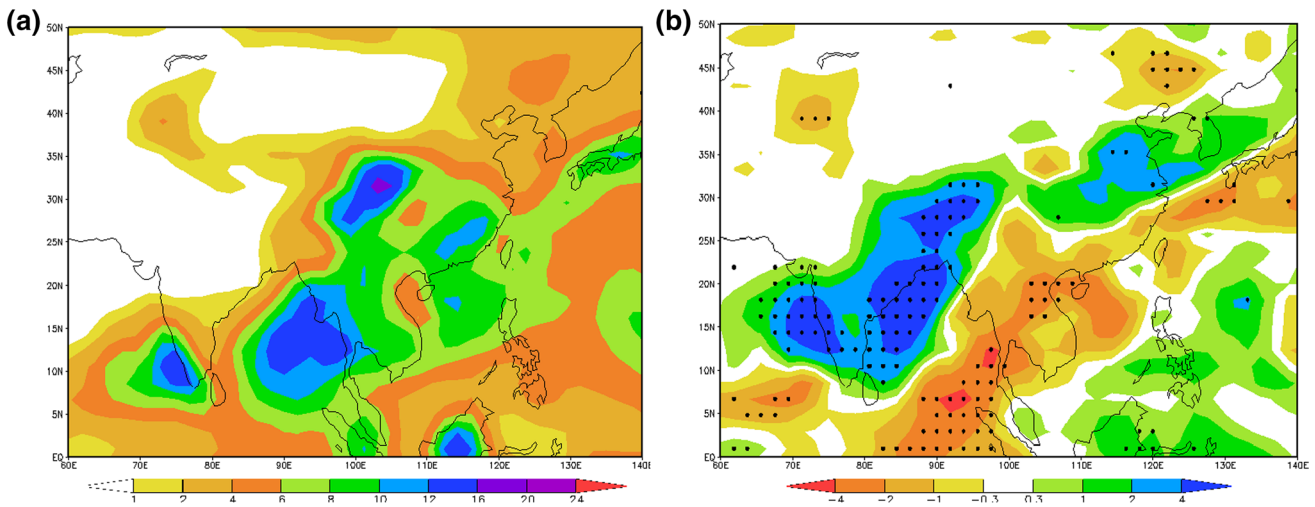

Fig. 18 **a** AMJ mean precipitation (mm day^{-1}) simulated from CTRL and **b** AMJ mean differences in precipitation between C1984 and CTRL for South/East Asia. The *dotted area* denotes differences which are statistically significant at a significance level of 0.1

has no impact on precipitation since the monsoon flow does not reach there and the Saharan desert is too dry to produce precipitation. On the other hand, the reduced upward air movement over the WAM region results in reduced precipitation. In South/East Asia, where the dust aerosols are overlapped with the rainfall band where moisture is sufficient, the anomalous heating of the upper air by the dust layers increases the upward motion and draws in more low-level moist air from the ocean and hence enhances the precipitation over the South/East Asian continental monsoon regions. Meanwhile, the rainfall over the ocean located to the south of the enhanced rainfall was reduced and generated a dipole pattern. Therefore, the dust aerosol effect on precipitation depends on the relative location of the dust with respect to the major rainfall band.

Wu et al. (2013) used WRF-Chem to study the aerosol effect on East Asian summer monsoon and reported that during the first phase of the monsoon (May–Mid-June), the precipitation occurs in southern China and the aerosols are located to the north of the precipitation. In that case, aerosol tends to reduce the precipitation over southern China. However, during the second phase of monsoon (Mid-June–Early August) when rainfall jumps northward to where the major aerosols are located, aerosol effect is to increase the precipitation over central-northern China. They attributed the increased precipitation during the second phase to both aerosol direct and indirect effects which cause a reduction of local cloudiness and induce ascent to the north and descent to the south, leading to a northward shift of precipitation and hence an increase of precipitation over central-northern China. They also claimed that the aerosol induced precipitation changes are mainly contributed by the anomalies in the vertical velocities, while the horizontal moisture flux plays a relatively small role. In our study, aerosol indirect effect is not included in the simulation. Therefore, the dust aerosol direct effect and the associated heating of the air column (semi-direct effect) appear to be responsible for the changes in circulation and precipitation. Different from their simulations which were only carried for 3 months for 2006 and 2007, respectively, JJAS mean precipitation in our simulations is increased in southern China because the model simulated climatology rainfall is located over southeastern China, while in their 2007 case, the major rainfall is located over central-northern China. Our simulations also show that the changes in moisture flux are important in the dust induced precipitation anomalies. To examine the precipitation change in the early phase of East Asian monsoon, Fig. 18 shows the April–May–June (AMJ) mean precipitation and the differences between C1984 and CTRL for South/Ease Asia. During the early phase of monsoon, precipitation mainly occurs over southeastern China around 25°N (Fig. 18a), while the dust particles are majorly located to the north over 30°N–40°N (Fig. 1). Due to the dust effect, precipitation decreases over southeastern China but increases over central to north China. In order to interpret the changes in precipitation pattern, Fig. 19 shows the AMJ mean temperature and streamlines at 115°E, where the maximum precipitation change is located over China, for CTRL and the differences between C1984 and CTRL. It is seen that deep tropical convection is located over equator to 5°N (Fig. 19a), corresponding to the center of precipitation over there (Fig. 18a). East Asia monsoon inflow starts at about 10°N and extends to about 35°N, where it is constrained by the subtropical high to the north (Fig. 19a). The dust particles produce warming in the middle troposphere and cooling over surface between

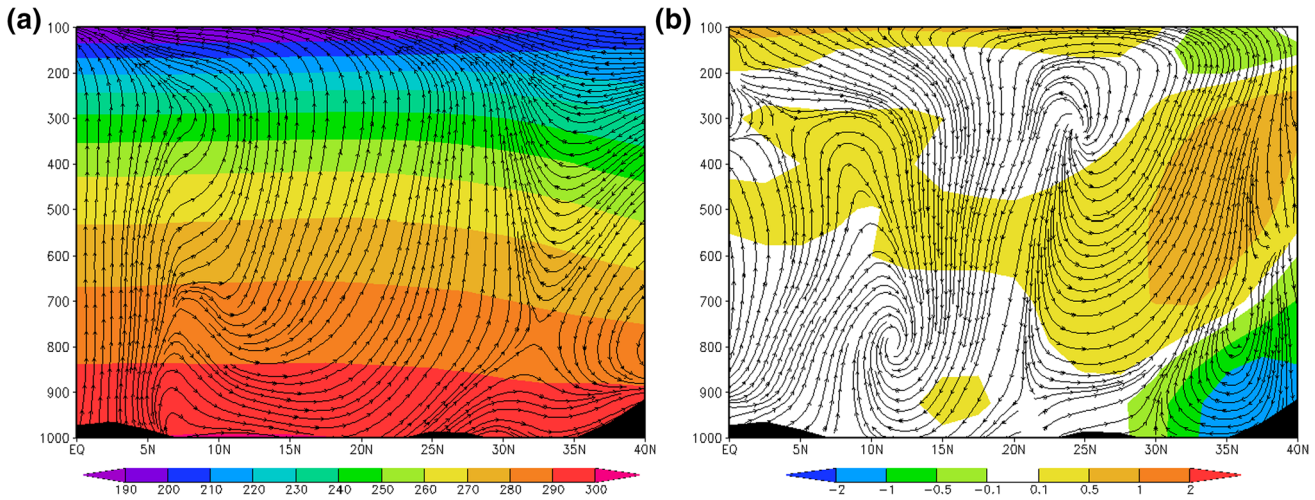

Fig. 19 Latitude-height cross section of AMJ mean **a** streamline (v; $-\omega \times 100$) and temperature (K, *shaded*), and **b** their differences between C1984 and CTRL at 115°E

30°N and 40°N (Fig. 19b). The warming in the atmosphere induces a stronger upward motion of the air at 25°N–30°N and an anomalous subsidence over 10°N–25°N, well corresponding to the increased/decreased precipitation over central-northern/Southeastern China. Therefore, during the early phase of the East Asia monsoon when the major monsoon precipitation occurs to the south of the dust location, dust heating effect to its north would draws the precipitation further inland, producing more precipitation over the dust location, but less precipitation over the major rainfall band. Different from the North Africa region, the central China is moist enough and the East Asia monsoon inflow is stronger than the WAM so that more precipitation could be produced when the heating of the atmosphere over there shifts monsoon circulation northward.

4 Conclusions

Climate simulations using the NCEP AGCM that incorporates a state-of-the-art land-surface scheme (SSiB2) have been carried out to investigate the role of dust aerosols on the precipitation over two major monsoon regions—North Africa/tropical North Atlantic and South/East Asia. 3D dust aerosol mixing ratio simulated from GOCART model for year 1984 and 2003 have been used, which represent relatively dry and wet scenarios, respectively.

Dust aerosols scatter and absorb substantial solar radiation, leading to the heating of the air column and decrease in solar flux reaching the surface. The effect of dust aerosols on regional climate, such as surface temperature and precipitation as well as circulation, has been examined for two major monsoon regions: North Africa and South/East Asia. The major difference between these two regions is that during monsoon season over North Africa, dust is mainly located to the north of the rainfall band, while over South/East Asia, dust is overlapped with the precipitation location. This difference affect where the dust heating happens with respect to the monsoon circulation and effect on the precipitation.

Decreases in surface temperature and sensible heat flux over the North Africa have been found due to dust effect. Due to the heating of the middle-upper troposphere by dust, the relative humidity and cloud cover (semi-direct effect) are reduced and OLR is increased; the upward vertical velocity increases over the dust region, leading to reduced upward motion to the south and weakened cyclonic circulation over the rainfall band. Therefore, precipitation decreases over Sahel area and tropical North Atlantic, located to the south of the major dust band.

Over the South/East Asia, dust aerosols are located where precipitation occurs, especially over the Southwest India and coastal area of the Bay of Bengal. Surface temperature and sensible heat flux also decrease due to the reduced downward solar flux. The heating of the upper atmosphere over the land and Tibetan Plateau enhances the upward vertical velocity and strengthens the cyclonic circulation over the precipitation band, which draws in more lower level moist air from the ocean, leading to increased cloud, decreased OLR, and increased precipitation over South/East Asia as a result of dust effect.

Decreases in surface temperature due to dust aerosols, which increases the stability relative to the surface, do not seem to play a dominant role in the changes of precipitation in South/East Asia. The heating of the air column due to dust particles, on the other hand, plays a major role. Dust aerosols act as a heating source in the atmosphere and generate an enhanced upward motion and a stronger

lower level convergence. In general, the dust heating effect would tend to intensify the monsoon precipitation if the dust layers overlap with the major monsoon rainfall band (such as in South Asia), or redistribute the precipitation more northward if the dust particles are located to the north of the monsoon rainfall band (e.g., in East Asia during early phase of Monsoon). When the air over the dust region is too dry and the monsoon circulation is unable to move northward due to the general circulation (e.g., North African Sahel and Sahara region), anomalous heating produced by the dust particles would not be able to shift the rainfall northward, but would reduce the precipitation over the major rainfall band. Meanwhile, by continuity, opposite vertical motion happens to the south of the areas where the precipitation change occurs. Therefore, whether the dust effect would enhance or suppress the precipitation depends on the location of the rainfall band with respect to the dust aerosols or the heating source and the circulation patterns associated with the precipitation. The dust effects are to modulate the regional circulation and redistribute the precipitation instead of simply reducing or enhancing the precipitation.

In the present study, the aerosol indirect effect on precipitation is not accounted for. The differences in precipitation distribution patterns, therefore, are associated with the interactions and feedback among aerosol, radiation, cloud, and dynamic fields which are modulated by the direct and semi-direct radiative forcings and in turn affect the simulated climate. The SST response to the aerosol forcing (Yue et al. 2011) is also ignored. Aerosol indirect effect and its effect through SST change may play an important role in convective cloud and incorporation of the aerosol indirect effect in the NCEP AGCM is a task we plan to accomplish in future endeavors.

Acknowledgments This research has been supported by NSF Grants AGS-1419526 and AGS-1115506, and DOE Grant DESC0006742. We thank Dr. Mian Chin at GSFC and Dr. Sarah Lu of the University at Albany, SUNY for their assistance in obtaining the aerosol single scattering properties associated with the GOCART data.

References

Andreae MO (1995) Climatic effects of changing atmospheric aerosol levels. In: Henderson-Sellers A (ed) World survey of climatology, vol 16, future climates of the world, Elsevier, New York, pp 341–392

Biasutti M, Giannini A (2006) Robust Sahel drying in response to late 20th century forcings. Geophys Res Lett 33:L11706. doi:10.1029/2006GL026067

Chin M, Ginoux P, Kinne S, Holben BN, Duncan BN, Martin RV, Logan JA, Higurashi A, Nakajima T (2002) Tropospheric aerosol optical thickness from the GOCART model and comparisons with satellite and sunphotometer measurements. J Atmos Sci 59:461–483

Chin M, Diehl T, Dubovik O, Eck TF, Holben BN, Sinyuk A, Streets DG (2009) Light absorption by pollution, dust, and biomass burning aerosols: a global model study and evaluation with AERONET measurements. Ann Geophys 27:3439–3464. doi:10.5194/angeo-27-3439-2009

Chou MD, Suarez MJ, Ho CH, Yan MMH, Lee KT (1998) Parameterizations for cloud overlapping and shortwave single-scattering properties for use in general circulation and cloud ensemble models. J Clim 11:202–214

Clark DB, Xue Y, Harding RJ, Valdes PJ (2001) Modeling the impact of land surface degradation on the climate of tropical North Africa. J Clim 14:1809–1822

Cook KH (1999) Generation of the African Easterly Jet and its role indetermining West African precipitation. J Clim 12:1165–1184

Cook KH, Vizy EK (2006) Coupled model simulations of the West African Monsoon System: twentieth- and twenty-first-century simulations. J Clim 19(15):3681–3703. doi:10.1175/JCLI3814.1

Das S, Dey S, Dash SK (2015) Impacts of aerosols on dynamics of Indian summer monsoon using a regional climate model. Clim Dyn 44:1685–1697. doi:10.1007/s00382-014-2284-4

Ding Y (1994) Monsoon in China. Kluwer Acad, Norwell

Engelstaedter S, Tegen I, Washington R (2006) North African dust emission and transport. Earth Sci Rev 79:73–100

Fels SB, Schwarzkopf MD (1975) The simplified exchange approximation: a new method for radiative transfer calculations. J Atmos Sci 32:1475–1488

Flohn H (1957) Large-scale aspects of the "summer monsoon" in South and east Asia. J Meteorol Soc Jpn 75:180–186

Ginoux P, Chin M, Tegen I, Prospero J, Holben B, Dubovik O, Lin SJ (2001) Sources and global distributions of dust aerosols simulated with the GOCART model. J Geophys Res 106:20255–20273

Griffiths JF (1972) General climatology. In: Griffiths JF (ed) Climates of Africa. Elsevier Sci, New York, pp 1–35

Gu Y, Liou KN, Xue Y, Mechoso CR, Li W, Luo Y (2006) Climatic effects of different aerosol types in China simulated by the UCLA general circulation model. J Geophys Res 111:D15201. doi:10.1029/2005JD006312

Gu Y, Liou KN, Chen W, Liao H (2010) Direct climate effect of black carbon in China and its impact on dust storm. J Geophys Res 115:D00K14. doi:10.1029/2009JD013427

Hansen J, Sato M, Ruedy R (1997) Radiative forcing and climate response. J Geophys Res 102:6831–6864

Hoerling M, Hurrell J, Eischeid J, Phillips A (2006) Detection and attribution of 20th century northern and southern African rainfall change. J Clim 19:3989–4008

Hou YT, Campana KA, Yang SK (1996) Shortwave radiation calculations in the NCEP's global model. In: International radiation symposium, IRS-96, August 19–24, Fairbanks, AL

Hou YT, Moorthi S, Campana KA (2002) Parameterization of solar radiation transfer in the NCEP models. NCEP Office Note, 441. http://www.emc.ncep.noaa.gov/officenotes/FullTOC.html#2000

Huang L, Jiang JH, Tackett JL, Su H, Fu R (2013) Seasonal and diurnal variations of aerosol extinction profile and type distribution from CALIPSO 5-year observations. J Geophys Res Atmos 118:4572–4596. doi:10.1002/jgrd.50407

Intergovernmental Panel on Climate Change (IPCC) (2007) The physical basis of climate change. Cambridge University Press, The Edinburgh Building Shaftesbury Road, Cambridge

Islam MN, Almazroui M (2012) Direct effects and feedback of desery dust on the climate of the Arabian Peninsula during the wet season: a regional climate model study. Clim Dyn 39:2239–2250. doi:10.1007/s00382-012-1293-4

Johnson BT, Shine K, Forster P (2004) The semi-direct aerosol effect: impact of absorbing aerosols on marine stratocumulus. Q J R Meteorol Soc 2004:1407–1422

Kanamitsu M, Ebisuzaki W, Woollen J, Yang SK, Hnilo JJ, Fiorino M, Potter GL (2002) NCEP-DOE AMIP-II reanalysis (R-2). Bull Am Meteorol Soc 83:1631–1643

Kim KM, Lau WK, Sud YC, Walker GK (2010) Influence of aerosol-radiative forcings on the diurnal and seasonal cycles of rainfall over West Africa and Eastern Atlantic Ocean using GCM simulations. Clim Dyn 35:115–126. doi:10.1007/s00382-010-0750-1

Köpke P, Hess M, Schult I, Shettle EP (1997) Global Aerosol Data Set (GADS). Max-Plank-Institute für Meteorologie, Report 243, Hamburg

Lamb PJ, Peppler RA (1992) Further case studies of tropical Atlantic surface atmospheric and oceanic patterns associated with sub-Saharan drought. J Clim 5:476–488

Lau KM, Kim MK, Kim KM (2006) Asian summer monsoon anomalies induced by aerosol direct forcing: the role of the Tibetan Plateau. Clim Dyn 26:855–864. doi:10.1007/s00382-006-0114-z

Lau KM, Kim KM, Sud YC, Walker GK (2009) A GCM study of the response of the atmospheric water cycle of Western Africa and the Atlantic to Saharan dust radiative forcing. Geophys Ann 27:4023–4037

Menon S, Hansen J, Nazarenko L, Luo Y (2002) Climate effects of black carbon aerosols in China and India. Science 297:2250–2253

Miller RL, Tegen I (1998) Climate response to soil dust aerosols. J Clim 11:3247–3267

Miller RL, Tegen I, Perlwitz J (2004) Surface radiative forcing by soil dust aerosols and the hydrologic cycle. J Geophys Res 109:D04203. doi:10.1029/2003JD004085

Nicholson SE (2000) Land surface processes and Sahel climate. Rev Geophys 38:117–139

Prospero JM, Ginoux P, Torres O, Nicholson SE, Gill TE (2002) Environmental characterization of global sources of atmospheric soil dust derived from the NIMBUS7 TOMS absorbing aerosol product. Rev Geophys 40:1002. doi:10.1029/2000RG000095

Ramanathan V, Chung C, Kim D, Bettge T, Buja L, Kiehl JT, Washington WM, Fu Q, Sikka DR, Wild M (2005) Atmospheric brown clouds: impacts on South Asian climate and hydrological cycle. PNAS 102:5326–5333

Redelsperger JL, Thorncroft CD, Diedhiou A, Lebel T, Parker DJ, Polcher J (2006) African monsoon multidisciplinary analysis: an international research project and field campaign. Bull Am Meteorol Soc 87:1739–1746

Rowell DP, Folland CK, Maskell K, Ward MN (1995) Variability of summer rainfall over tropical North Africa (1906–1992): observations and modeling. Q J R Meteorol Soc 121:669–704

Satheesh SK, Moorthy K (2005) Radiative effects of natural aerosols: a review. Atmos Environ 39:2089–2110

Schwarzkopf MD, Fels SB (1991) The simplified exchange method revisited: an accurate, rapid method for computation of infrared cooling rates and fluxes. J Geophys Res 96(D5):9075–9096

Stevens B (2013) Uncertain then, irrelevant now. Nature 503:47–48

Sun H, Pan Z, Liu X (2012) Numerical simulation of spatial-temporal distribution of dust aerosol and its direct radiative effects on East Asian climate. J Geophys Res 117:D13206. doi:10.1029/2011JD017219

Taylor CM, Lambin EF, Stephenne N, Harding RJ, Essery RLH (2002) The influence of land use change on climate in the Sahel. J Clim 15:3615–3629

Vinoj V, Rasch PJ, Wang H, Yoon JH, Ma PL, Landu K, Singh B (2014) Short-term modulation of Indian summer monsoon rainfall by West Asian dust. Nat Geosci. doi:10.1038/NGEO2107

Webster PJ, Magana V, Palmer TN, Shukla J, Tomas RA, Yanai M, Yasunari T (1998) Monsoons: processes, predictability, and the prospects for prediction. J Geophys Res 103(C7):14451–14510

Wu L, Su H, Jiang JH (2013) Regional simulation of aerosol impacts on precipitation during the East Asian summer monsoon. J Geophys Res 118:6454–6467

Xu KM, Randall DA (1996) A semi-empirical cloudiness parameterization for use in climate models. J Atmos Sci 53:3084–3102

Xue Y (1997) Biosphere feedback on regional climate in tropical North Africa. Q J R Meteorol Soc 123:1483–1515

Xue Y, Shukla J (1993) The influence of land surface properties on Sahel climate. Part I: desertification. J Clim 6:2232–2245

Xue Y, Sellers PJ, Kinter JL III, Shukla J (1991) A simplified biosphere model for global climate studies. J Clim 4:345–364

Xue Y, Juang HMH, Li WP, Prince S, DeFries R, Jiao Y, Vasic R (2004) Role pf land surface processes in monsoon development: east Asia and West Africa. J Grophys Res 109:D03105. doi:10.1029/2003JD003556

Xue Y, De Sales F, Lau KM, Boone A, Feng J, Dirmeyer P, Guo Z, Kim KM, Kitoh A, Kumar V, Poccard-Leclercq I, Mahowald N, Moufouma-Okia W, Pegion P, Rowell D, Schubert SD, Sealy A, Thiaw WM, Vintzileos Williams AS, Wu ML (2010) Intercomparison and analyses of the climatology of the West African monsoon in the West African Monsoon Modeling and Evaluation Project (WAMME) first model intercomparison experiment in special issue "West African monsoon and its modeling". Clim Dyn 35:3- 27. doi:10.1007/s00382-010-0778-2

Xue Y, De Sales F, Lau WK-M, Boone A, Kim K-M, Chin M, Comer R, Druyan lM, Dirmeyer P, Gu Y, Hagos SM, Hosaka M, Kalnay E, Kito A, Koster R, Kucharsk F, Leung R, Mahanama S, Mahowald NM, Mechoso CR, Rowell D, Schiro K, Seidou Sanda I, Thiaw W, Wang G, Zhang Z, Zeng N (2015) West African monsoon decadal variability and surface-related forcings: Second West African Monsoon Modeling and Evaluation Project Experiment (WAMME II). In this special issue

Yoshioka M, Mahowald NM, Conley AJ, Collins WD, Fillmore DW, Zender CS, Coleman DB (2007) Impact of desert dust radiative forcing on Sahel precipitation: relative importance of dust compared to sea surface temperature variations, vegetation changes, and greenhouse gas warming. J Clim 20:1445–1467

Yue X, Wang H, Liao H, Fan K (2010) Simulation of dust aerosol radiative feedback using the GMOD: 2; dust-climate interactions. J Geophys Res 115:D04201. doi:10.1029/2009JD012063

Yue X, Liao H, Wang H, Li SL, Tang JP (2011) Role of sea surface temperature responses in simulation of the climatic effect of mineral dust aerosol. Atmos Chem Phys 11:6049–6062

Zhan X, Xue Y, Collatz GJ (2003) An analytical approach for estimating CO_2 and heat fluxes over the Amazonian region. Ecol Model 162:97–117

Zhao C, Liu X, Leung LR, Hagos S (2011) The radiative impact of mineral dust onhydrological cycles during the monsoon season over West Africa. Atmos Chem Phys 11:1879–1893